

Table 1. Direction of interaction in doublets

	V1→V1	V1→V2	V1→V4	V2→V1	V2→V2	V2→V4	V4→V1	V4→V2	V4→V4
Mean±SEM (%)	12.3±3.9 (622.5±142.0)	9.3±2.3 (208.4±61.2)	5.0±1.3 (219.5±79.8)	8.3±1.3 (230.0±32.4)	26.7±7.3 (934.8±337.0)	9.5±3.1 (118.2±43.0)	6.3±1.3 (253.7±72.3)	9.0±2.0 (192.7±90.6)	13.6±3.9 (328.2±112.7)
Mean±SEM (%)	21.8±5.7 (395.6±195.5)	22.0±5.9*	15.9±3.1*	4.4±1.3*	10.0±2.0*	4.5±1.3*	7.9±2.7 (115.1±64.4)	8.0±2.1 (61.5±20.7)	5.5±1.0* (47.2±19.3)
Mean±SEM (%)	15.1±2.1 (31.9±13.7)	9.4±1.2 (16.2±6.9)	8.3±1.8 (10.0±3.8)	8.5±1.5 (11.3±4.2)	12.1±2.0* (39.2±15.2)	7.4±2.6 (5.8±2.8)	15.7±2.6* (13.4±5.1)	9.5±2.4 (6.7±3.0)	14.0±3.3 (10.7±4.5)

Table 1: Upper row shows the significantly repeating doublets in stimulus-evoked trials; middle row shows the significantly repeating doublets in fixation-only trials; bottom row shows the most informative doublets (as defined in the main text). The upper number in each row is the normalized percentage of doublets per trial; the number in brackets in each row is the actual count of doublets per trial (note that the actual counts are not normalized and they strongly depend on the number of imaged pixels within each area; counts appear as Mean±SEM, averaged over 9 imaging sessions). The normalized percentage of doublets was calculated by dividing the number of the significantly repeating doublets found within a single area or between two areas, by the square number of pixels within a single area or the product of the number of pixels composing each of the two areas, respectively. The distribution within each condition was then normalized to 100%. The variability among imaging sessions can be attributed mainly to staining quality and different animals.

When we compared the fraction of doublets found in stimulus-evoked vs. blank (stimulus-free) trials, we found significant difference in most of the doublets groups (marked with an asterisk in the middle row; Wilcoxon rank-sum test, $p<0.005$). When we compared the fraction of the whole population of doublets vs. the most informative ones (both found in stimulus-evoked trials), we found significant difference in (V2→V2) and (V4→V1) groups (marked with an asterisk in the bottom row; Wilcoxon rank-sum test, $p<0.005$).

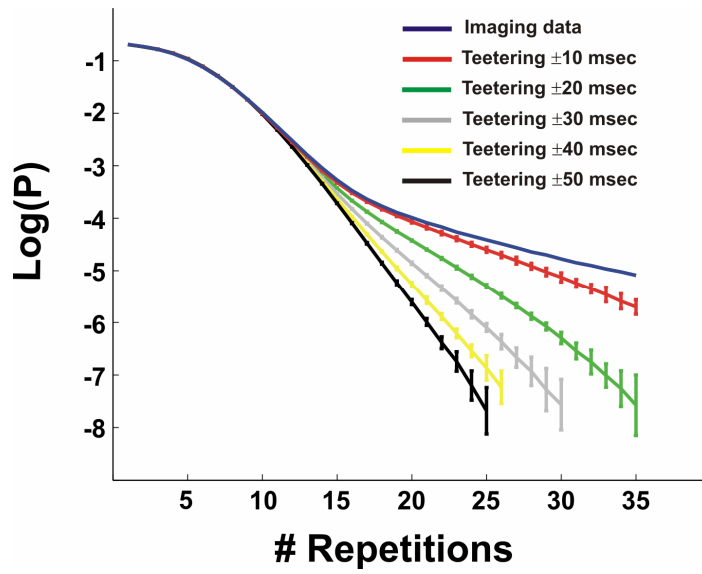


Figure S1. Real data and surrogates at different teetering windows

Example of the probability density function (*pdf*) of doublet-repetition count for one imaging session and its corresponding teetering surrogates on a log scale. Blue trace denotes the *pdf* of the imaging data; other traces denote the mean *pdf* of the surrogate data created by teetering the PEs within a $\pm(10-50)$ msec time window. Error bars denote $\pm 2 \times \text{SD}$ calculated over 25 generated surrogates.

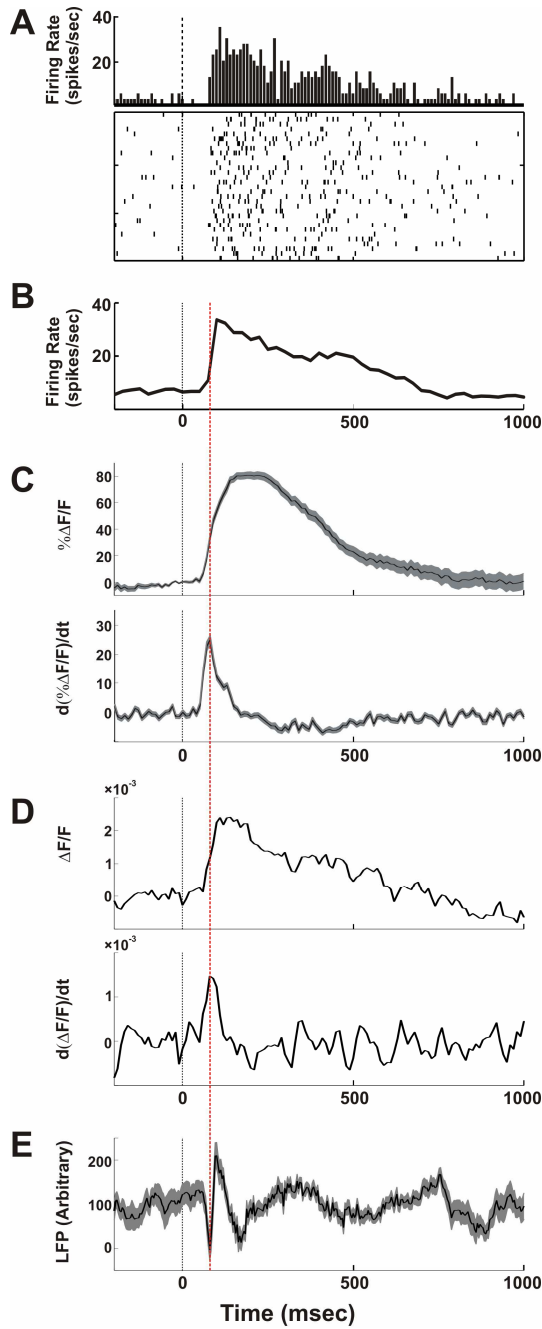


Figure S2. Comparing spiking activity, LFP and VSDI activation

A, Example of one single-unit spiking activity evoked by a stimulus consisting of a collinear array of three Gabors. The neuron's receptive field was centered on the middle Gabor, and the Gabor's orientation was adjusted to the neuron's preferred orientation. The upper panel depicts the post-stimulus time histogram (PSTH), computed in 10 msec bins, and the lower panel shows the raster plots of 31 trials. **B,** Population activity of all recorded units (19 single units and 30 multi-units, bin size = 10 msec), visual stimulus

as in A. **C**, Upper panel shows the evoked VSDI response amplitude for the same visual stimulus as in A, averaged over 75 pixels at the center of activation (*i.e.*, these pixels corresponded to populations of neurons having receptive fields located at the center of the Gabor). The activity was averaged over 8 recording sessions (102 trials, mean \pm SEM). Lower panel shows the first derivative of VSDI amplitude in a 20 msec sliding time window (*i.e.* the difference between time points 20 msec apart). **D**, Upper and lower panels show the same signals as in C only for one single pixel (located in the center of the activation) in one single trial. **E**, Mean LFP signal evoked by the same stimulus as in A, recorded from a single electrode located in the center of the Gabor (31 trials, mean \pm SEM). Red dashed line depicts the time of the VSDI derivative maximum and the LFP signal minimum.

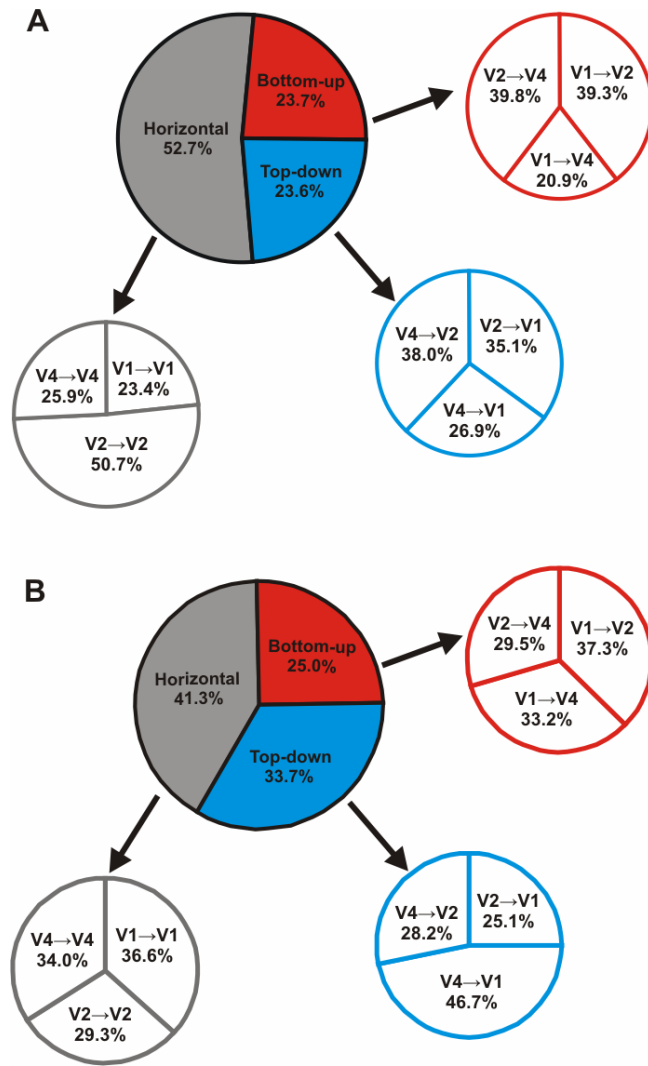


Figure S3. Summary of the direction of interaction in doublets

A, Frequency of doublet groups: doublets extending within a single cortical area (V1, V2 and V4); bottom-up doublets (V1→V2), (V1→V4) and (V2→V4); top-down doublets (V2→V1), (V4→V1) and (V4→V2). Data were averaged over 9 imaging sessions. **B**, Same as A, only for the most informative doublets (as defined in the main text).

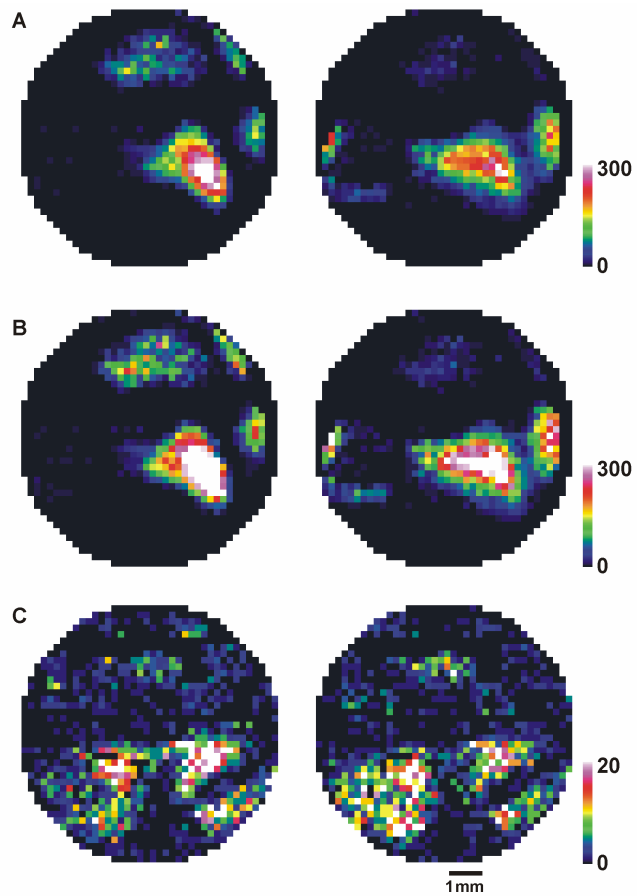


Figure S4. Spatial clustering of doublets

Spatial clustering of the significantly repeating doublets occurring in different visual stimuli. Each map counts the number of doublets that either start (left panel) or end (right panel) at a given pixel (*i.e.* this pixel is the locus of either the first or the second PE in the doublet). A to C depict the coherent face-stimulus, the scrambled stimulus and the blank condition, respectively. Data were taken from a single imaging session.

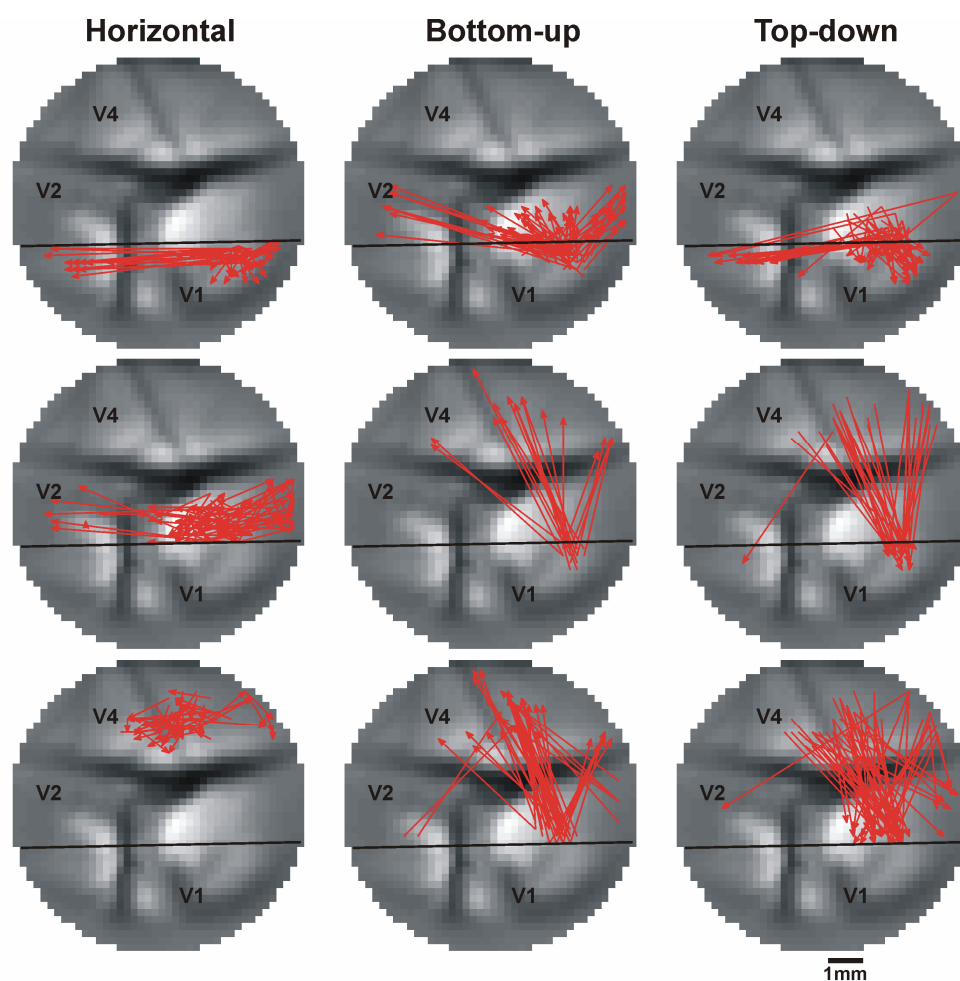


Figure S5. Representative doublets significantly repeating in scrambled face-stimulus

Representative doublets significantly repeating in scrambled face-stimulus trials of a single imaging session. Each doublet is represented as an arrow drawn between the pixels sequentially activated in the pattern. From top to bottom: Left column shows examples of horizontal doublets extending within V1, V2 and V4; middle column shows examples of bottom-up doublets ($V1 \rightarrow V2$), ($V1 \rightarrow V4$) and ($V2 \rightarrow V4$); right column shows examples of top-down doublets ($V2 \rightarrow V1$), ($V4 \rightarrow V1$) and ($V4 \rightarrow V2$).

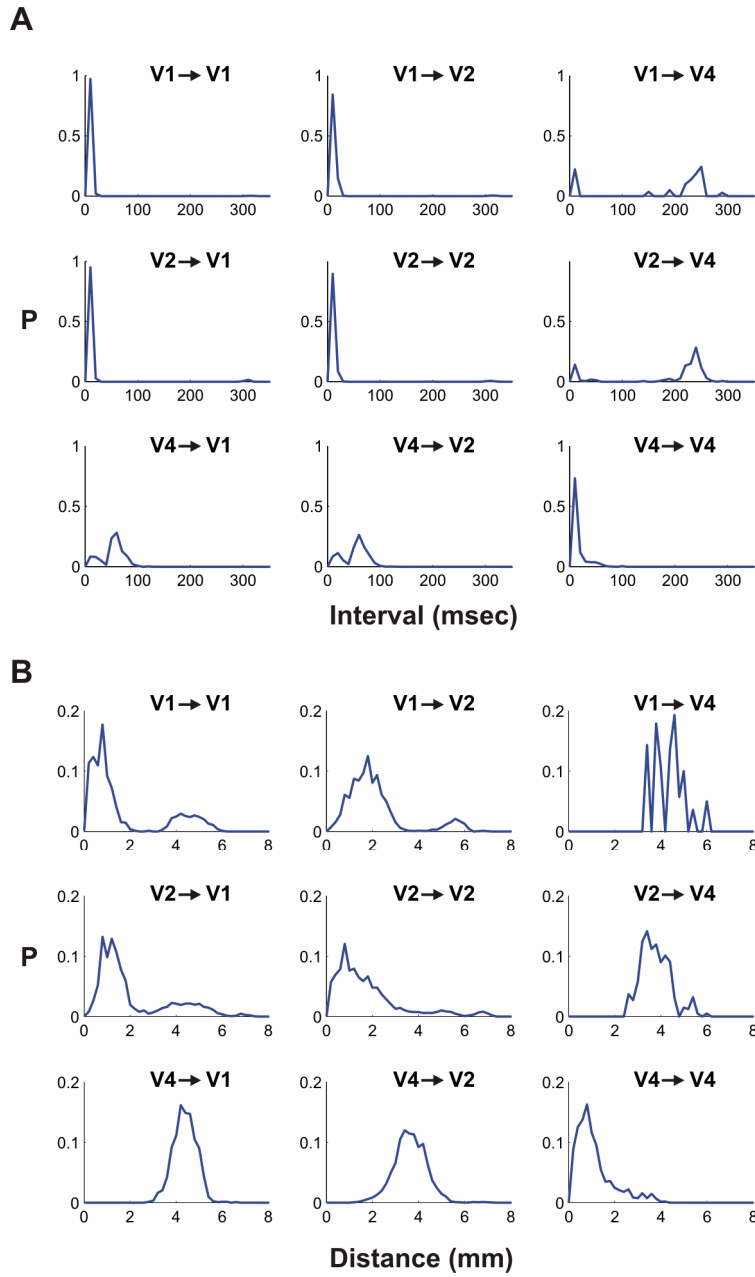


Figure S6. Doublet characteristics within cortical regions

A, The *pdf* of doublet interval within a single cortical area (V1, V2, V4) and between each area, shown for each combination. **B**, The *pdf* of doublet distance within a single cortical area and between each area, shown for each combination. Data taken from a single imaging session; doublets were detected after removal of mean stimulus contribution.

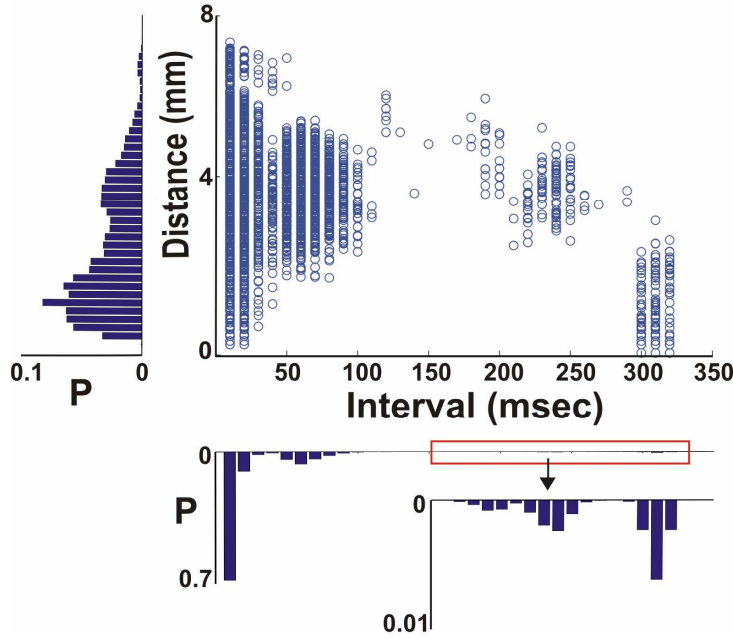


Figure S7. Doublet characteristics: the relation between distance and time interval

Scatter plot of doublet distance vs. doublet interval from a single imaging session. The *pdf*s of the doublet interval and distance are plotted along the *x*- and *y*-axes of the scatter plot respectively. Four distinct hills can be seen: (a) a high peak of short intervals (10-30 msec), corresponding mainly to doublets within V1, within V2 and between V1-V2; (b) a wide hill around intervals of 50-100 msec, corresponding mainly to top-down doublets going from V4 to the lower areas V1 and V2; (c) a very low and spread-out hill around intervals of 180-260 msec, corresponding to bottom-up doublets going from V1, V2 to V4; (d) another low hill around intervals of 300-320 msec, corresponding mainly to doublets within V2.

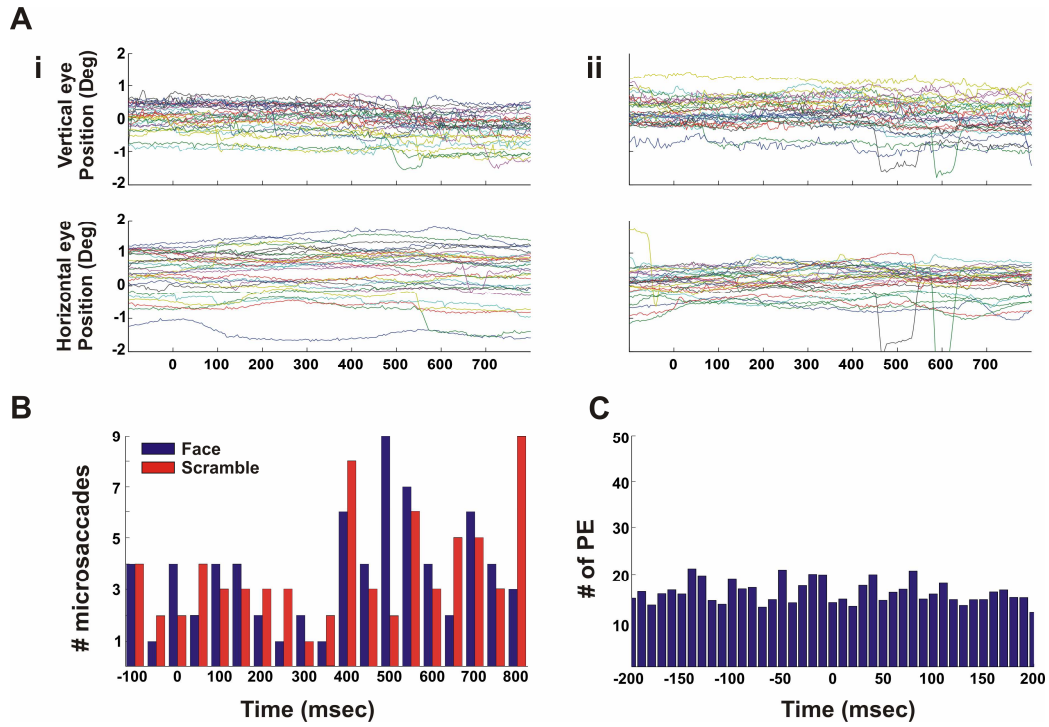


Figure S8. Eye movements

A, Example of eye movements during one imaging session. **(i)** Face-stimulus trials ($n=28$); **(ii)** Scrambled-stimulus trials ($n=28$). **B**, Time histogram of microsaccades, calculated in 50 msec bins for the data in A. Note that the rate of microsaccades (or small saccades) increases only around 400 msec after visual-stimulus onset, *i.e.*, 100 msec after visual-stimulus offset. The histogram shows no significant difference in the microsaccade patterns between the face and the scrambled stimulus (Wilcoxon rank-sum test, $p>0.05$). **C**, Discrete time-event histogram triggered on microsaccades averaged over 28 trials and 71 microsaccades. The flat histogram indicates that the microsaccades did not induce any event modulation in the VSDI signal that could induce an excess of spatio-temporal patterns.

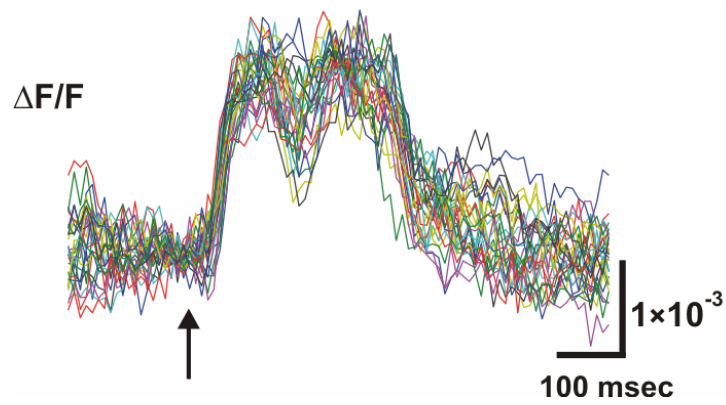


Figure S9. VSDI amplitude Variability

Example of the time course of VSDI response amplitude in a face-stimulus experiment (consisting of 28 trials, averaged over 15 pixels in V1), demonstrating the variability of the neural-population response across trials. Black arrow denotes stimulus onset.

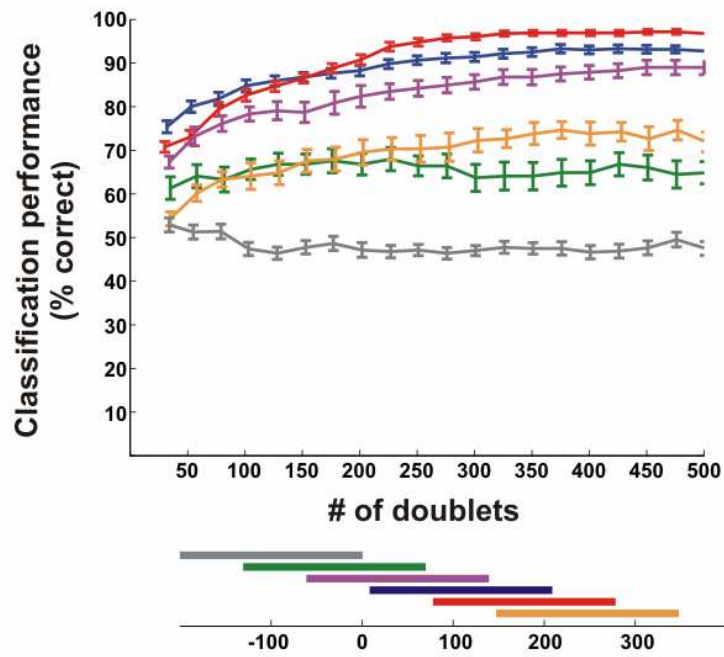


Figure S10. Comparing readout performance using doublets occurring in different time windows

Performance of binary k -NN classifier as a function of the number of doublets used for the readout within various time windows (specified in the bottom panel). For every classification experiment, we chose doublets occurring within a 200 msec time window.

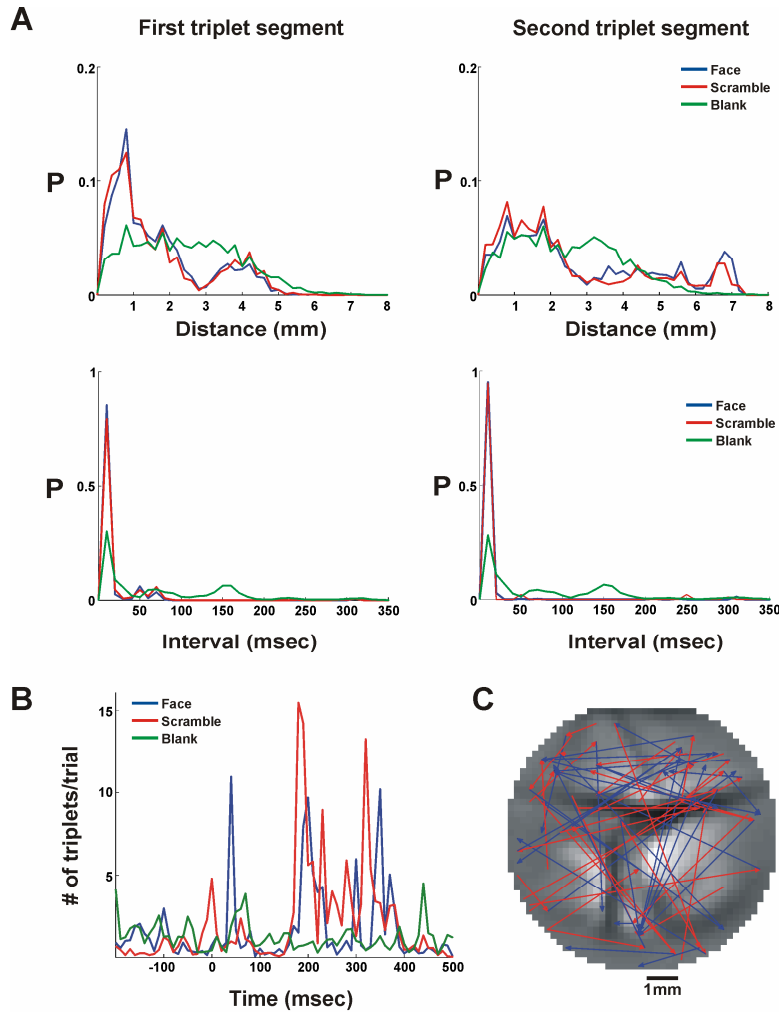


Figure S11. Triplets statistics

A, The *pdf*s of distance (upper panels) and time-intervals (lower panels) of the first and second segments of the triplets (left and right panels, respectively), that significantly repeat in trials belonging to coherent-face, scrambled-face and blank conditions. Both the triplet interval and the triplet distance exhibit no significant difference between the scramble and the face stimuli, and both exhibit a significant difference between the stimulus and the blank (Wilcoxon rank-sum test, $p < 0.005$). **B**, PSTH of the significantly repeating triplet occurrences in a single imaging session; blue, red and green traces depict face, scrambled and blank trials, respectively. **C**, Representative triplets significantly repeating in blank trials. The triplets shown here were chosen randomly from a single imaging session, making up ~2% of all the significantly repeating triplets. Data in A-C were taken from a single imaging session.

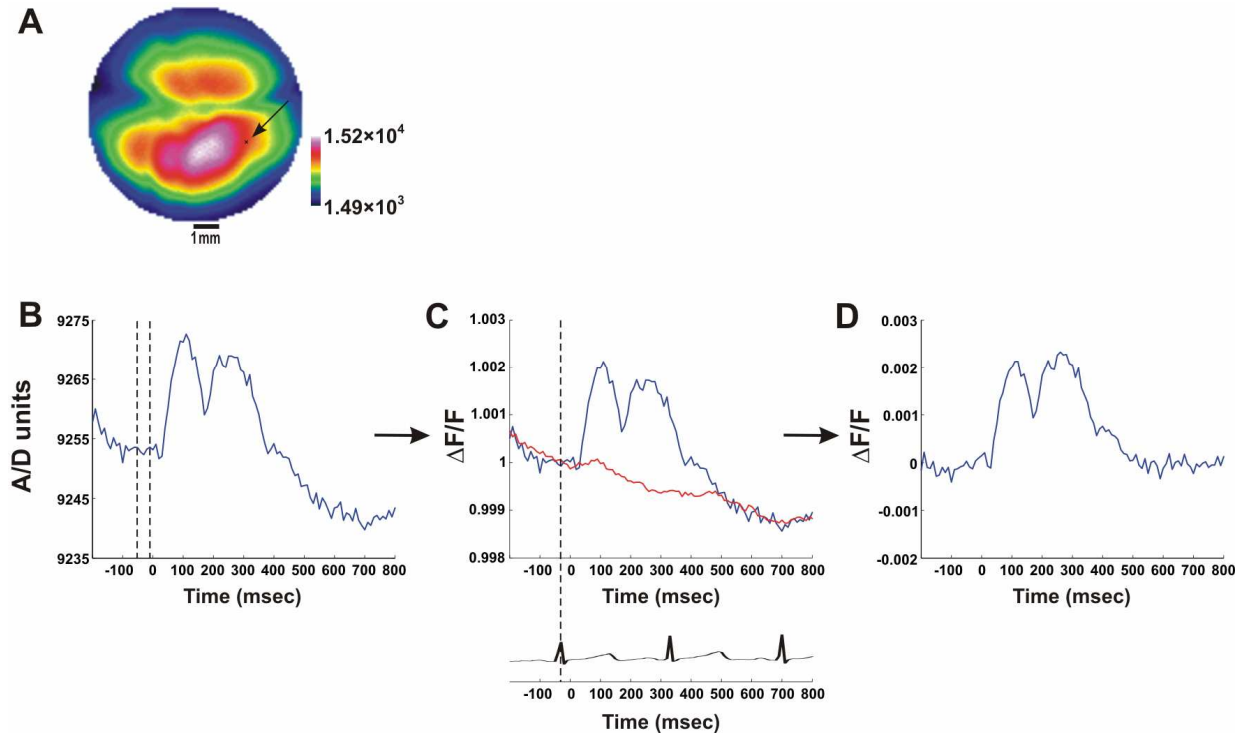


Figure S12. Schematic illustration of VSDI basic-analysis

A, A typical pattern of illumination map acquired from one VSDI session. The map shows the fluorescence intensity (in A/D units) measured from each pixel within the imaged area. Only pixels with illumination level $\geq 15\%$ (the pixel with the highest illumination value was considered 100%) were analyzed. The arrow points to a pixel that is illustrated in parts B to D of this figure. **B**, The raw VSDI signal of one pixel (marked with an arrow in A) in one stimulus-evoked trial. The Y-axis shows the A/D units that correspond to fluorescence intensity level. The dashed lines depict the frame range used to compute the average background-fluorescence. **C**, Upper panel: Blue trace depicts the VSDI signal of the same pixel shown in A, after background-fluorescence division (*i.e.* normalized to background-fluorescence). Red trace depicts the VSDI signal of the same pixel in the normalized average blank (stimulus-free, fixation-only). Lower panel depicts the ECG signal of one trial synchronized with the VSDI data-acquisition and with the stimulus onset. **D**, The normalized VSDI signal of the same pixel, after the subtraction of the average blank.

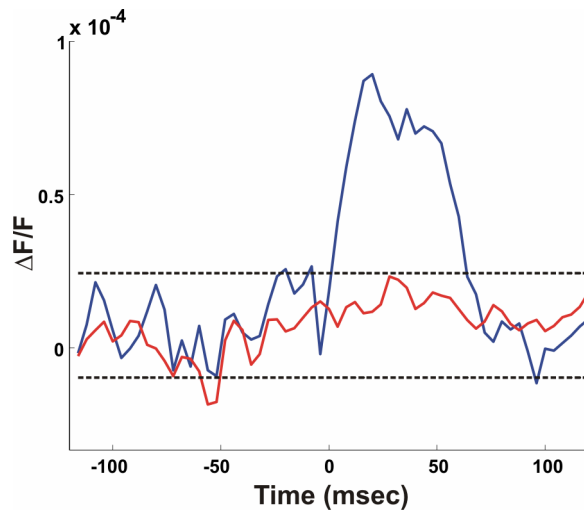


Figure S13. Doublet-triggered average (DTA), showing no significant evidence of oscillatory activity around doublet occurrence

The average VSDI signal triggered on the significantly repeating doublet in stimulus-evoked activity, after subtraction of mean-stimulus response (averaged over all the significantly repeating doublets found in 558 pixels of V1 area of one imaging session which was recorded at 4 msec/frame). Blue trace depicts the DTA of the optical signal; red trace represents the shuffle condition: DTA of the VSDI with doublet shuffling between trials. The dashed black lines represent $\pm 2 \times \text{STD}$ from the mean of the shuffle condition (the red trace).